ISSN 2354-9114 (online), ISSN 0024-9521 (print)
Indonesian Journal of Geography Vol 56, No 3 (2024): 435-444
DOI: 10.22146/ijg.89225 website: https://jurnal.ugm.ac.id/ijg

INDONESIAN JOURNAL OF GEOGRAPHY

RESEARCH ARTICLE

Use of HAND Model for Estimating Flood-Prone in Serawai Basins Base on Remote Sensing and Sistem Information Geography

***Ajun Purwanto[1], Dony Andrasmoro[2], Eviliyanto[3]**
[1,2,3] Department of Geography Education , IKIP PGRI Pontianak

Received: 2023-09-22
Revised: 2024-05-31
Accepted: 2024-09-20
Published: 2024-12-03

Key words: HAND Model; Estimating; Geospatial; Flood-Prone; Watershed

Correspondent email: ajunpurwanto@ikippgriptk.ac.id

Abstract. A river basin's flood-prone mapping is essential for managing flood risks, developing mitigation plans, and developing flood forecasting and warning systems, among other things. This research uses the HAND model to estimate the level of flood-prone and its distribution in watersheds. The method used is survey and image interpretation. The data used is DEM imagery with a resolution of 10 meters. Data analysis uses spatial analysis, which includes elevation, hydrological analysis, fill, flow accumulation, flow direction, flow distance, and minus statistical analysis. The results showed that the Serawai watershed has five classes: very prone, prone, moderate, not prone, and very not prone. The very prone class has an area of 112,213.82 ha (65.41%), including Tontang, Sedaha, Nanga Serawai, Begori, Nanga Lekawai, Surga, Buntut Ponte, and Nanga Segulang village. The prone class has an area of 29,356.65 ha (17.14%), spread across the village of part of Beurgea, part of Nanga Segulang, Nanga Jelundung, and part of Tontang village. The moderate level has an area of 18,971.52 ha (11.08%), spread across Tontang, part of Nanga Jelundung, and part of Baras Nabun village. The area with a not-prone is 7,996.20 ha (4.67%), spread across Baras Nabun and parts of Nanga Jelundung village. For areas that are very not prone, they have an area of 3,004.20 (1.75%), spread over parts of the villages of Sedaha, parts of Baras Nabun, and Nanga Jelundung. Based on the research results, it can be concluded that the HAND Model is an effective and easy-to-use model for estimating flood-prone areas.

1. Introduction

Flood is a natural process that has occurred worldwide, even before human existence itself, and has been a decisive factor in the rise and development of civilizations and the decadence of others (Dantas & Paz, 2021; Goerl et al., 2017). One of the calamities that frequently affects different parts of Indonesia is flooding. Given that Indonesia is a tropical region with heavy rainfall, floods are a reasonable occurrence. The impact of these catastrophic calamities on human lives is tremendous. Flooding is one of the most pervasive natural hazards that negatively impacts too many aspects, such as social (Geographic, 2019; Rincón et al., 2018), including loss of human life and adverse effects on the population, damage to the infrastructure, and essential services, damage to crops and animals, the spread of diseases, and contamination of the water supply (Rincón et al., 2018). High yearly rainfall raises sea levels and river bottoms, resulting in floods in many different world regions. Over the past three decades, floods have considerably increased everywhere (Komolafe et al., 2020; Rozalis et al., 2010).

Many factors cause flooding, such as climate change (Ozkan & Tarhan, 2016; Zhou et al., 2021), soil structure and type (Jha et al., 2011; Zwenzner & Voigt, 2009), sparse vegetation, slope, and people (Hu & Demir, 2021). Another cause is land use change, such as deforestation and urbanization (Ekmekcioğlu et al., 2021; Huong & Pathirana, 2013; Rincón et al., 2018; Zhang et al., 2018; Zhou et al., 2021). Floods are also caused by hydrological conditions such as the capacity of river channels to convey flood flows, geological characteristics related to structure and rock types, and complex geomorphological processes, such as significant changes in river channels (Cendrero et al., 2022; Gentile et al., 2022; Gorczyca et al., 2014; Prokop et al., 2020; Rączkowska et al., 2024), resulting in major environmental damage (Gorczyca et al., 2014; Komolafe et al., 2020; Mukherjee & Singh, 2020; Purwanto et al., 2022; Skilodimou et al., 2019). The impacts of floods include loss of human life, damage to infrastructure, destruction of crops and animals, loss of ecosystem services, spread of disease, and contamination of water supplies (Rincón et al., 2018)

The most unpredictable natural calamities, floods, must be avoided entirely; they cannot be partly stopped. Its incidence may be predicted, and the damage can be minimized with practical risk assessment. In recent years, a growing body of studies on flood risk assessment and analysis has been carried out in different regions and cities both in the lowlands end coastal areas (Cai et al., 2021; Sarmah et al., 2020), comparatively little investigation has been performed on the upstream area which is a mountainous region. An area in the mountain cities is sensitive to sudden floods due to significant elevation disparity and other specific factors (Romanescu et al., 2018).

The West Kalimantan region's sub-districts have experienced significant flooding due to excessive rains. One of them is in Sintang Regency's Serawai District. As a result of heavy rains, the Melawi river water overflowed and caused a

flood of water to rise to the villages in Sabang Landan Village, Tontang Village, Temakung Village, Tanjung Harapan Village, Pagar Lebata Village, Bedaha Village, Talian Sahabung Village, Begori Village, Gurung Sengiang Village, Batu Ketebung Village, Tanjung Raya Village, Nanga Serawai Village, Tanjung Baru Village, Mentatai Village, Nusa Tujuh Village, Nanga Tekungai Village, Segulang Village and Baras Nabun Village. Even a few months ago, the flood reached a height of 2 meters to 3.5 meters, which resulted in many residents having to evacuate.

When considering the more frequent occurrence of intense and extreme weather events, such as floods (Coumou & Rahmstorf, 2012), it is of critical importance to develop an understanding and means of effectively predicting inundation extent, the central aspect of hydrological hazard. Various technologies, including Remote Sensing and Geographic Information Systems, have also been developed for monitoring flood disasters. Remote Sensing has contributed substantially to flood monitoring and damage assessment, leading disaster management authorities to contribute significantly (Haq et al., 2012), and the Geographical Information System. Numerous methods have been developed to map flood risk, extent, and damage evaluation. The goal is to be used as a guide for the operation of Remote Sensing (RS) and Geographic Information Systems (GIS) to improve the efficiency of monitoring and managing flood disasters (Haq et al., 2012).

A river basin's flood-prone mapping is essential for managing flood risks, developing mitigation plans, and developing flood forecasting and warning systems, among other things. One approach for this mapping is based on the HAND (Height Above Nearest Drainage), directly derived from the Digital Elevation Model (DEM), in which each pixel represents the elevation difference of this point about the river drainage network to which it is connected (Dantas & Paz, 2021).

HAND is an analysis approach directly derived from DEM, involving two other products also extracted from DEM: the flow directions and the drainage network (Dantas & Paz, 2021; Forner et al., 2015). This study uses the HAND model to estimate the level of flood-prone and its distribution in watersheds

2. The Method

Study Area

This research was conducted in the Serawai Watershed, Sintang Regency, West Kalimantan Province, Indonesia, located between longitude 112°25'00" E - 112°46'30" E and latitude 0°30'00" S - 0°45'00" S (Figure 1). The study area is approximately 171.542,39 ha. The Serawai watershed includes Sabang Landan Village, Tontang Village, Temakung Village, Tanjung Harapan Village, Pagar Lebata Village, Bedaha Village, Talian Sahabung Village, Begori Villages, Gurung Sengiang Village, Batu Ketebung Village, Tanjung Raya Village, Nanga Serawai Village, Tanjung Baru Village, Mentatai Village, Nusa Seven Village, Nanga Tekungai Village, Segulang Village and Baras Nabun Village.

Method

The method used in this research is survey and image interpretation. The data used include: a) Topographic maps and DEM (Digital Elevation Model) images with a resolution of 10 meters from ALOS Palsar. Some of the data collected in this study are:

a. Land Use Land Cover

Land use land cover data was generated from Sentinel 2A Land Cover. LULC causes changes to the natural drainage system (Mehr & Akdegirmen, 2021; Sugianto et al., 2022), impacts surface runoff, and affects infiltration capacity (Mehr & Akdegirmen, 2021). These

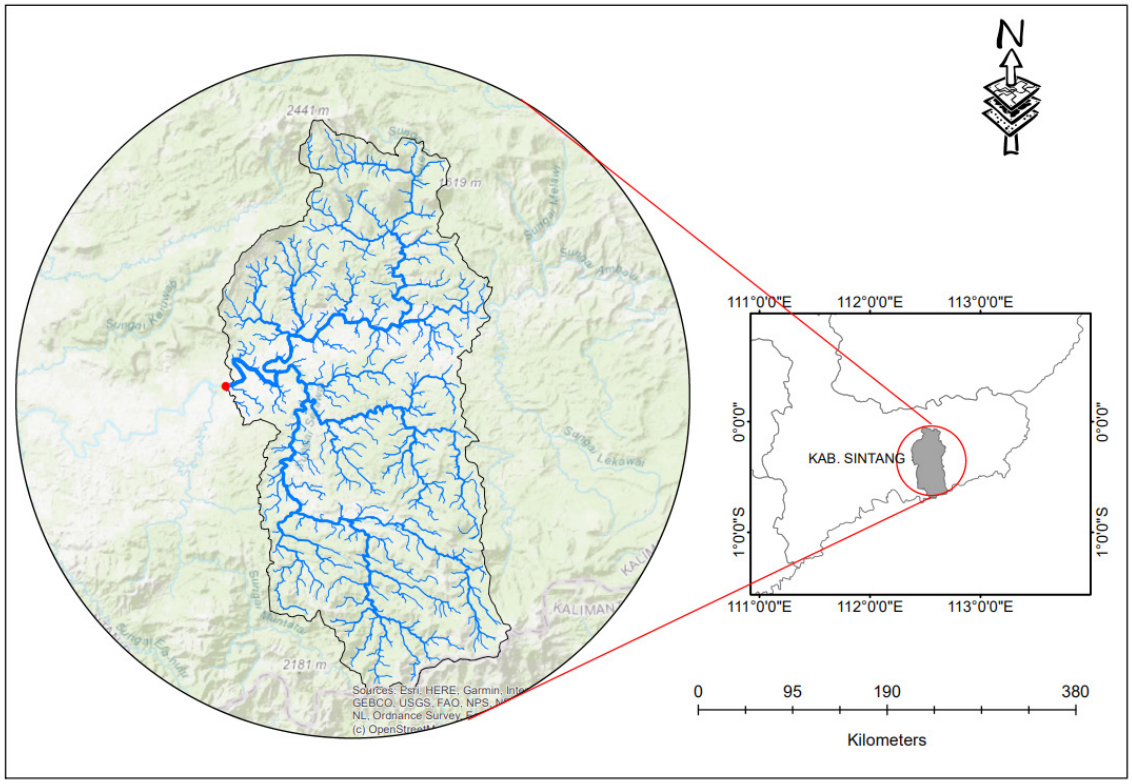

Figure 1. Study Area

factors are believed to be the cause of frequent flooding. Meanwhile, the level of available vegetation cover and infiltration rate also change the evapotranspiration rate (Hu & Demir, 2021). These factors alter the behavior and balance that occurs between water evaporation (Sugianto et al., 2022), water absorption (Nahib et al., 2021), and water distribution through rivers (Nahib et al., 2021; Sahoo et al., 2018). The result of the land cover analysis of the Serawai sub-watershed can be seen in Figure 3.

b. Basic Digital Elevation Model processing

The study area's basic digital altitude model processing is processed to obtain a basic information layer for estimating the flood area. The flow direction is established after any depressions have been eliminated, i.e., each pixel's flow direction is given to one of its eight neighbors (D8 - Deterministic Eight-Neighbor technique) (Dantas & Paz, 2021; Jenson & Domingue, 1988; Mark, 1984).

The primary guideline for choosing the direction of flow is to point it in the direction of the neighboring pixel with the highest slope. However, there are also particular guidelines for treating depressions and planes depending on the algorithm, which typically involves changing the height (Barnes et al., 2014). The flow direction determines the accumulated drainage area. This area comprises a raster layer with each pixel's attribute representing an upstream contribution area, the total of all the pixel areas whose flow routes lead to that pixel.

c. Slope

The slope is an important indicator of flood-prone surface zones (Alemayehu, 2007; Wondim, 2016). Slope affects the speed at which water flows through drainage channels and watersheds (Hu & Demir, 2021). In addition, the steeper the slope, the higher the water runoff; consequently, a higher peak discharge will be generated. The 0-8% slope class occupies most of the watershed, meaning that most of the watershed is highly vulnerable to flood hazards. This is because steep slopes are more prone to surface runoff, while flatlands are prone to waterlogging. Water moves more slowly, collects over a longer period, and accumulates on fatter surfaces, making them more susceptible to flooding than steeper surfaces (Desalegn & Mulu, 2021; Gigović et al., 2017; Hagos et al., 2022; Rimba et al., 2017; Singh et al., 2020; Wondim, 2016).

d. Hydrological Characteristics

The drainage network is established based on the cumulative drainage area, which is calculated by applying a threshold to the accumulated area (Fan et al., 2013; Goerl et al., 2017; Momo et al., 2016; Speckhann et al., 2018). In other words, network drainage is represented by all watershed pixels, with drainage areas more significant than the threshold. Different threshold values that reflect the drainage network's sensitivity are more than or equal to 100. Several morphometric analyses were carried out in this study, among others Perimeter (P), Compactness

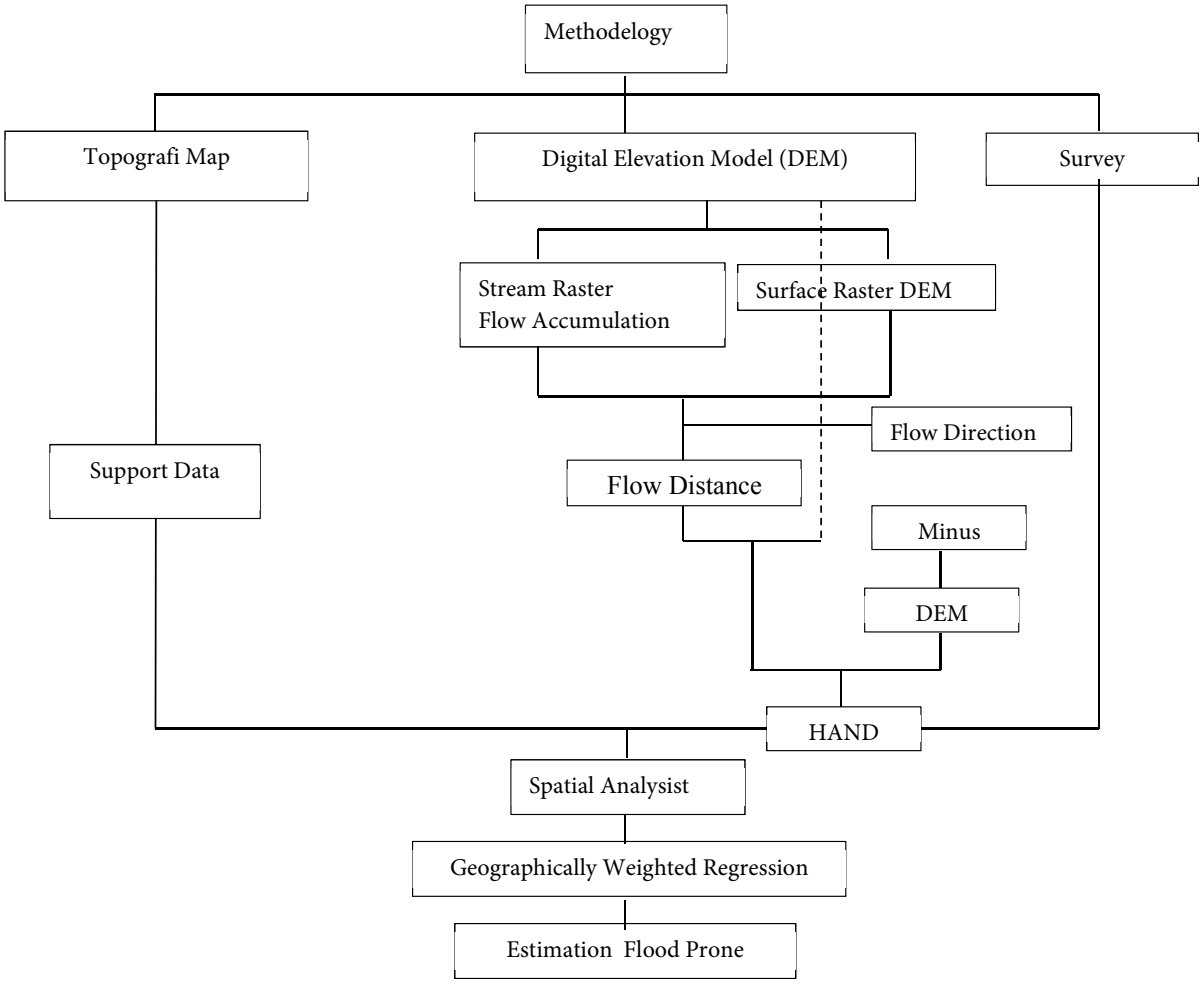

Figure 2. Research Method

Coefficient (Cc), Form Ratio (Fr), Circularity Racio (Rc), Drainage density (Dd) (Cardoso et al., 2006; Santos et al., 2021).

e. Soil

Soil is one of the essential factors for delineating the groundwater potential in study areas. Soil characteristics can control rates of infiltration, percolation, and permeability (Burayu, 2022; Purwanto & Andrasmoro, 2023). Grain size and types influenced the ability to control infiltration, percolation, and permeability rates (Kumar et al., 2021; Sajil Kumar et al., 2022).

f. Combining existing vector drainage networks

DEM processing technique, known as stream flaring, has been used to define the flow route in a manner compatible with the vector network's representation of the DEM river drainage network (Lindsay, 2016; Wu et al., 2019). With the exact DEM spatial resolution, the vector network has transformed to a raster format, and DEM pixels directly adjacent to the vector network's representative pixels are height reduced. As with DEMs without river burning, this burnt DEM is processed to derive flow directions, accumulation areas, basin borders, and drainage networks while removing basins.

ArcGIS 10.8 is utilized, which contains a DEM processing system, to determine HAND terrain descriptors in the form of flow directions, basin borders, and drainage networks formatted as raster. The topography reference of HAND changes (Dantas & Paz, 2021; Nobre et al., 2011), and a corresponding referential (Zr) is assigned to each pixel. HAND is determined based on the difference between Zp and Zr. Estimating the flood area is carried out in a standard way, namely by reclassifying the HAND value with scoring and classifying flood hazards from very prone, prone, moderate, non-prone, and very non-prone. The stages of the research methodology can be seen in Figure 2.

Data analysis

Data analysis used spatial analysis which included elevation, slope, and hydrological analysis including filling, flow accumulation, flow direction, and flow distance, minus statistical analysis, as well as sub-watershed morphometric analysis. In addition, it also uses reclassify analysis to determine the research area's level of flood proneness. For data exploration using ArcGis 10.8.

Table 1. Land Cover Serawai Sub-Watershed

Land Use Land Cover	Area (Ha)
Water Body	1.142,24
Forest	158.222,47
Flooded Vegetation	22,08
Field	78,97
Built Area	156,55
Shrubs	5.735,57
Bareland	1.994,27

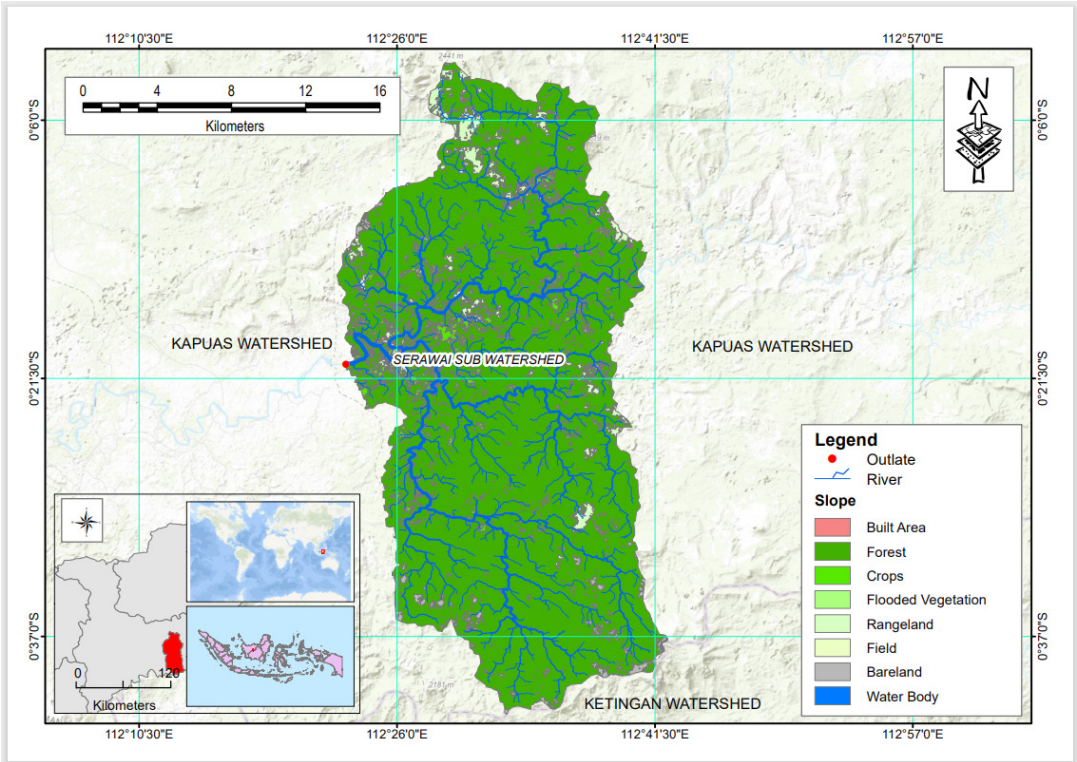

Figure 3. Land Use Land Cover Serawai Sub Watershed

3. Result and Discussion

Land Use Land Cover

The results of the analysis of land cover data generated from Sentinel 2A land use land cover known as sub-watershed land cover can be seen in Table 1.

Based on the data in Table 1, it is known that forest land use land cover has the most extensive area, namely 158.222,47 Ha, followed by shrub land 5.735,57 Ha, while bare land has an area of 1.994,27 HA. Land cover greatly influences flood-prone and determines the amount of stormwater runoff that exceeds the infiltration rate. Land that is heavily vegetated increases the infiltration rate of stormwater and slows down the time it takes for stormwater runoff to reach the river. This reduces the likelihood of flooding compared to unvegetated areas (J. Liu et al., 2018; Ullah & Zhang, 2020).

Elevation

The primary determinant of floods is altitude. Flood incidents generally increase with decreasing height due to the height's influence (Choubin et al., 2019; Mumbai, 2020). It is proven that places with low elevations often experience flooding every rainy season. The DEM in this study provides altitude information processed with ArcGIS 10.8. The height factor and slope angle are classified into five classes (Althuwaynee et al., 2012; Bui et al., 2019). Flooding is more likely to occur in low-altitude, flat locations with low slopes. The digital elevation maps are edited to factor elevations using the reclassify command in ArcGIS 10.8. Furthermore, this layer is divided into five classes 0 - 45, 45 - 107, 107 - 160, 160 - 206, and 206 - 254 m.

In the research area, flooding happens along rivers. As a result, another geomorphologically linked conditioning element is the distance from the river. Additionally, a map of the distance from the river is created since the river flow will affect the slope's stability by cutting the river's foot or soaking some of the material beneath the water's surface (Mojaddadi et al., 2017). River proximity and drainage indicate the distance from the river.

Hydrological Characteristic

The digital river map was edited using Euclidean with ArcGIS 10.8 to create a distance factor layer from the river. This order is further divided into five classes, namely orders 1, 2, 3, 4, 5, and 6. The region's distribution and intensity of floods are significantly influenced by the distance from the river (or by the distance of the measuring site from the river) (Bui et al., 2019; Grayson & Ladson, 1991). In areas with insufficient infiltration and percolation due to changes in soil characteristics, vegetation cover, and slope of the land surface, high-intensity rainfall events produce large amounts of runoff around nearby rivers, thus causing major flood disasters in downstream areas, with lower topographical gradients (Bui et al., 2019; Kia et al., 2012).

Several morphometric analyses were conducted in this study for the preliminary evaluation of flood probability. In this study, we calculated the morphometric parameters to evaluate the Serawai sub-watershed using the formula proposed by (Cardoso et al., 2006; Santos et al., 2021) as presented below.

Compactness coefficient (Cc)

$$C_c = 0.28\frac{P}{\sqrt{A}} \quad \text{.....(1)}$$

Where P is the basin perimeter (km), and A is the basin area (km^2).

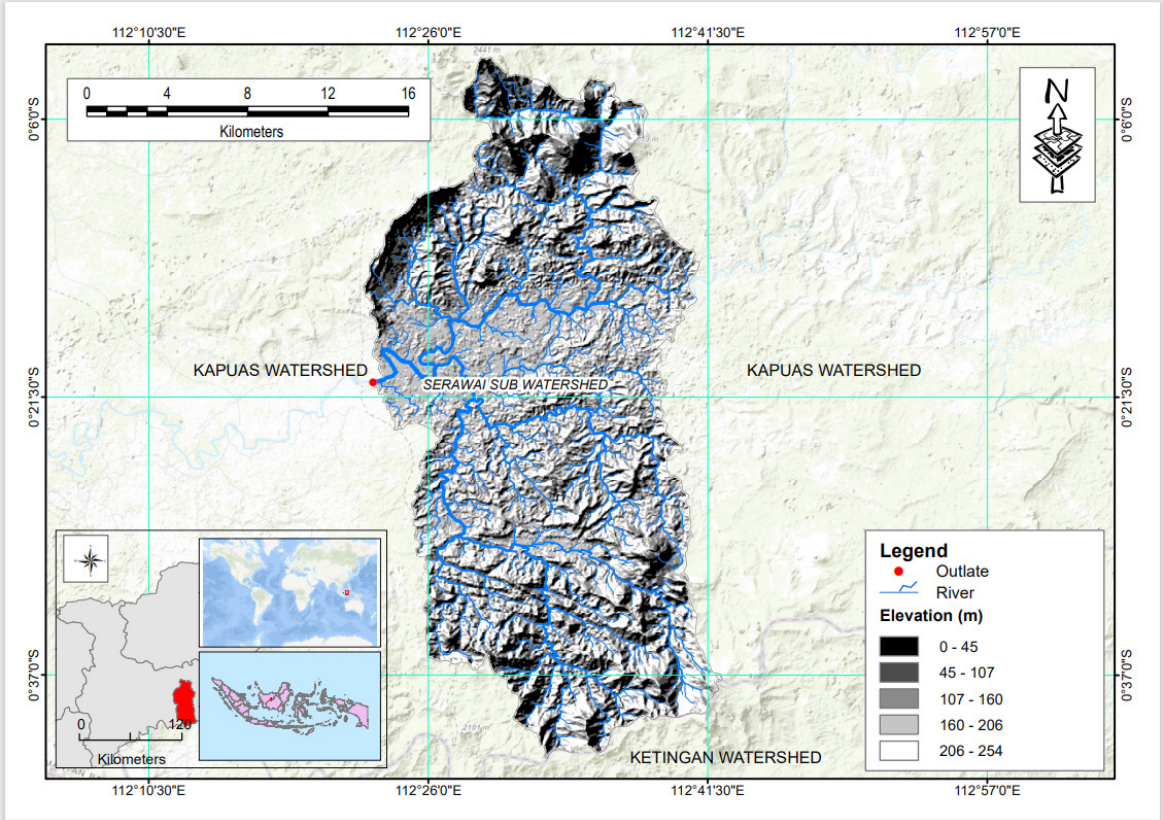

Figure 4. Sub-Watershed Elevation

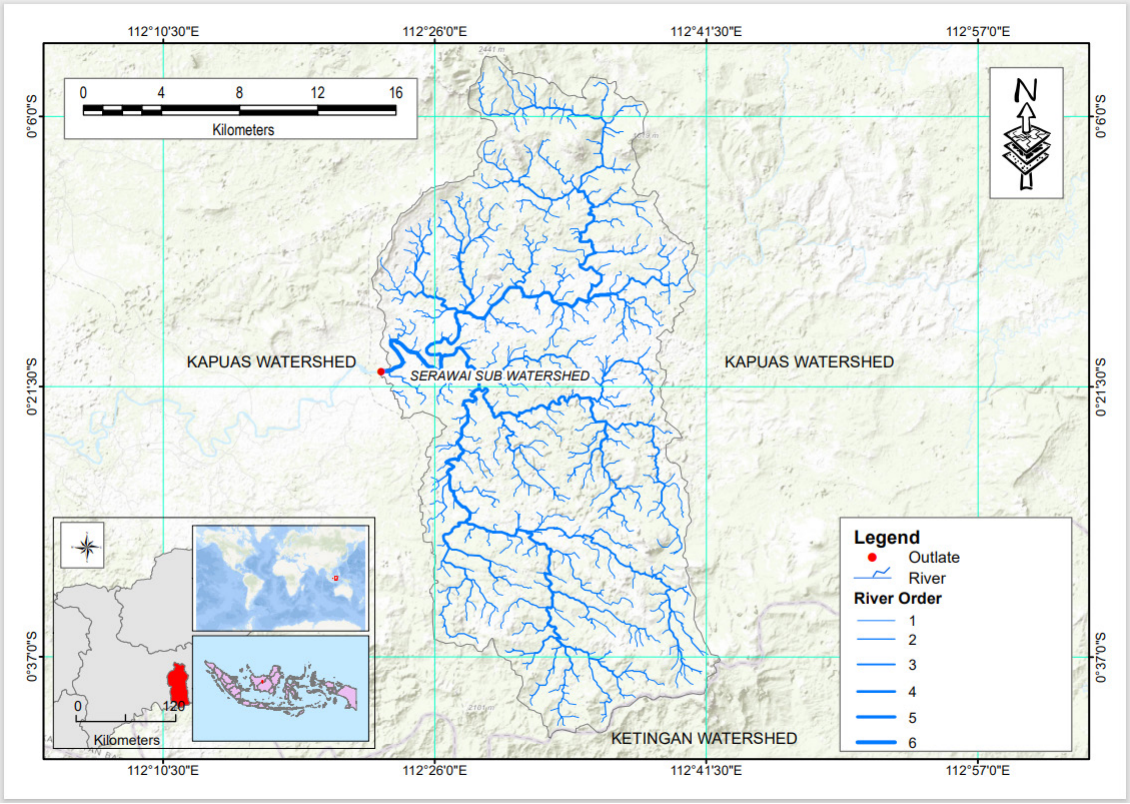

Figure 5. Flow Pattern

Table 2. Morphometric parameters of the Serawai Sub Watershed

Parameter	Serawai Sub Watershed
Area	1.715,42 Km^2
Perimeter	239,47 Km
Compactness Coefficient (Cc)	1,618
Form Ratio (Fr)	0,001
Circularity Racio (Rc)	0,376
Drainage density (Dd)	0,761

Form ratio (Ff)

$$F_f = \frac{A}{L^2} \quad \text{.....(2)}$$

Where, A is the basin area (km^2), and L is the basin length (km).

Circularity ratio (Rc)

$$R_C = \frac{12,57A}{P^2} \quad \text{.....(3)}$$

Where, A is the basin area (km2), and P is the basin perimeter (km).

Drainage density (Dd)

$$D_d = \frac{L}{A} \quad \text{.....(4)}$$

Where L is the total stream length (km), and A is the basin area (km^2)

Based on the above formula, the hydrological characteristics of the study area can be seen in Table 2.

If the Compactness coefficient ($C_C = 1$) the watershed tends to have a circular shape, resulting in large water overflows from the main river, thereby increasing flood vulnerability (Santos et al., 2021). The Serawai sub-watershed has a compactness coefficient of 1.618, which indicates an irregular shape, so it is not susceptible to flooding. The form ratio shows that the sub-watershed has a rectangular shape. It is defined as the ratio of the average basin width to the axial length (Cardoso et al., 2006). The analyzed watershed has a relatively low Form ratio (Ff = 0.001), indicating a low flood tendency. Similar to the Compactness Coefficient, Circularity Racio shows the similarity of the watershed shape to a circle shape; values close to 1 indicate circularity, and values greater than 1, extension (Cardoso et al., 2006; Santos et al., 2021). The obtained Racio Circularity (Rc = 0.367 also characterizes a low probability/ probability of flooding. Drainage density indicates the time required for rainfall to leave the basin; That is, it indicates the efficiency of the drainage system. According to (Santos et al., 2021) poorly drained basins have a drainage density of around 0.5 km/km2, while well-drained basins show values close to or greater than 3.5 km/km2. The Serawai Sub-watershed is shown to have moderate drainage capacity (Dd = 0.761 km/km2). For other hydrographic characteristics namely, river flow patterns, what exists is a dendritic pattern

Soil greatly influences flooding because of its ability to absorb water, which is called infiltration. Studies examine factors that influence infiltration, including in Aceh, West Kalimantan Province, Indonesia (Basri & Chandra, 2021; Purwanto et al., 2022; Silalahi et al., 2019; Suryadi & Riduansyah, 2021). Physical factors include soil texture, structure, and density. The study area is dominated by ultisol soil which has a clay texture. This land is also easily flooded due to its low ability to drain water (Y. Liu et al., 2019). The link between soil and flooding is the ability to absorb water, a process called infiltration. Physical factors that influence infiltration include soil texture, structure, and density. Coarse-textured soil has a greater infiltration capacity than fine-textured soil. Soil with low structure and density has faster infiltration than soil with high structure and density. Rapid infiltration reduces the risk of flooding because the overlying flooded soil drains more quickly vertically. The type of soil in the study area can be seen in Figure 6.

Geographic Information System (GIS) software, namely ArcGIS 10.8, is used to generate the HAND model by employing flow direction and flow distance data that has been processed using the Minus tool with the assistance of DEM to obtain HAND. The results showed that the Serawai watershed has five prone classes: very prone, prone, moderate, not prone, and very not prone.

Based on the results of the HAND analysis of the distribution and extent of flood risk, it can be seen in Table 3.

The very prone class has an area of 112,213.82 ha (65.41%), this area is very prone to flooding because the area is dominated by flat topography, with a low slope, medium river density, and a soil type dominated by clay texture, so infiltration is low. Areas with a high level of prone have an area of 29,356.65 ha (17.14%). Areas with a high level of moderate in general are also because they are located on flat to wavy topography, river density is moderate and the soil texture is dominated by clay. The moderately prone level has an area of 18,971.52 ha (11.08%), due to being located on a sloping topography, the soil is dominated by clay texture but the density of rivers is rare. The area that is not prone is 7,996.20 ha (4.67%), while in very non-prone areas it has an area of 3,004.20 (1.75%). This condition is because this area is in a hilly topography.

The very prone class spread over the villages of Tontang, Sedaha, Nanga Serawai, Begori, Nanga Lekawai, Surgaa, Buntut Ponte, and Nanga Segulang. Areas with a high level of prone are spread across the villages of part of Beurgea, part of Nanga Segulang, Nanga Jelundung, and part of Tontang village. The

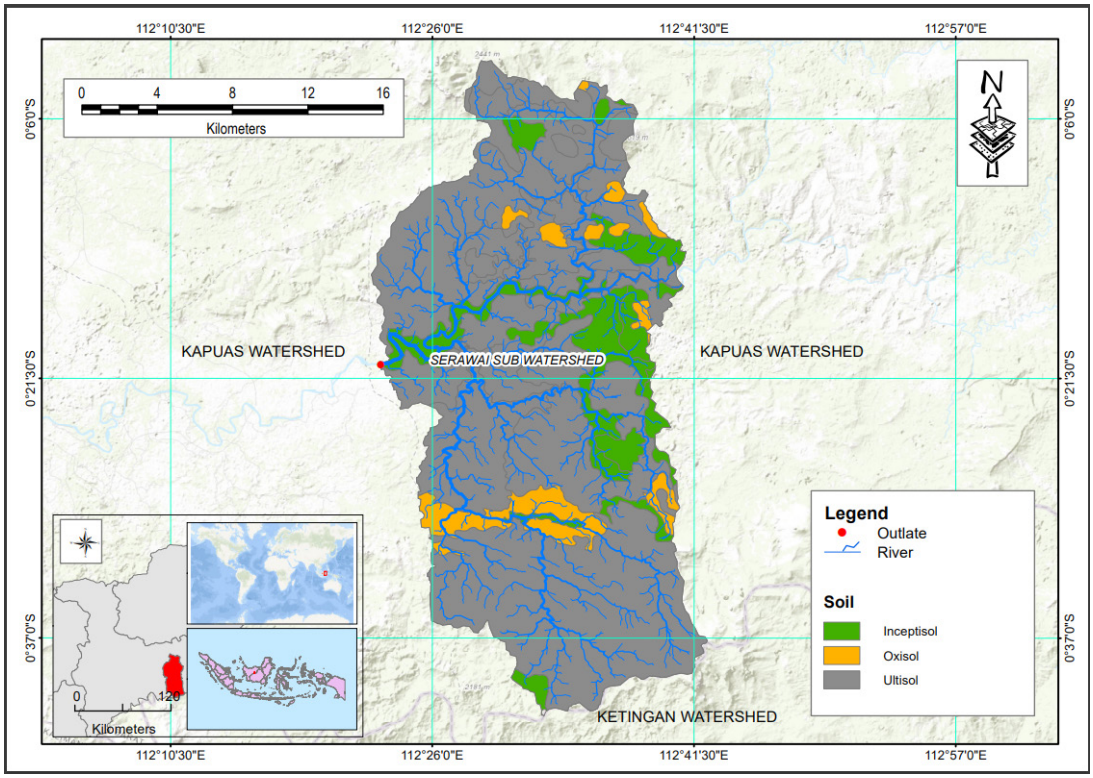

Figure 6. Soil Type

Table 3. Area and Percentage of Flood Prone

Prone Classes	Area (ha)	%
Very prone	112,213.82	65.41
Prone	29,356.65	17.11
Moderate	18,971.52	11.06
Not prone	7,996.20	4.66
Very not prone	3,004.20	1.75
Sum	171,542.39	100,00

Source: secondary data processing

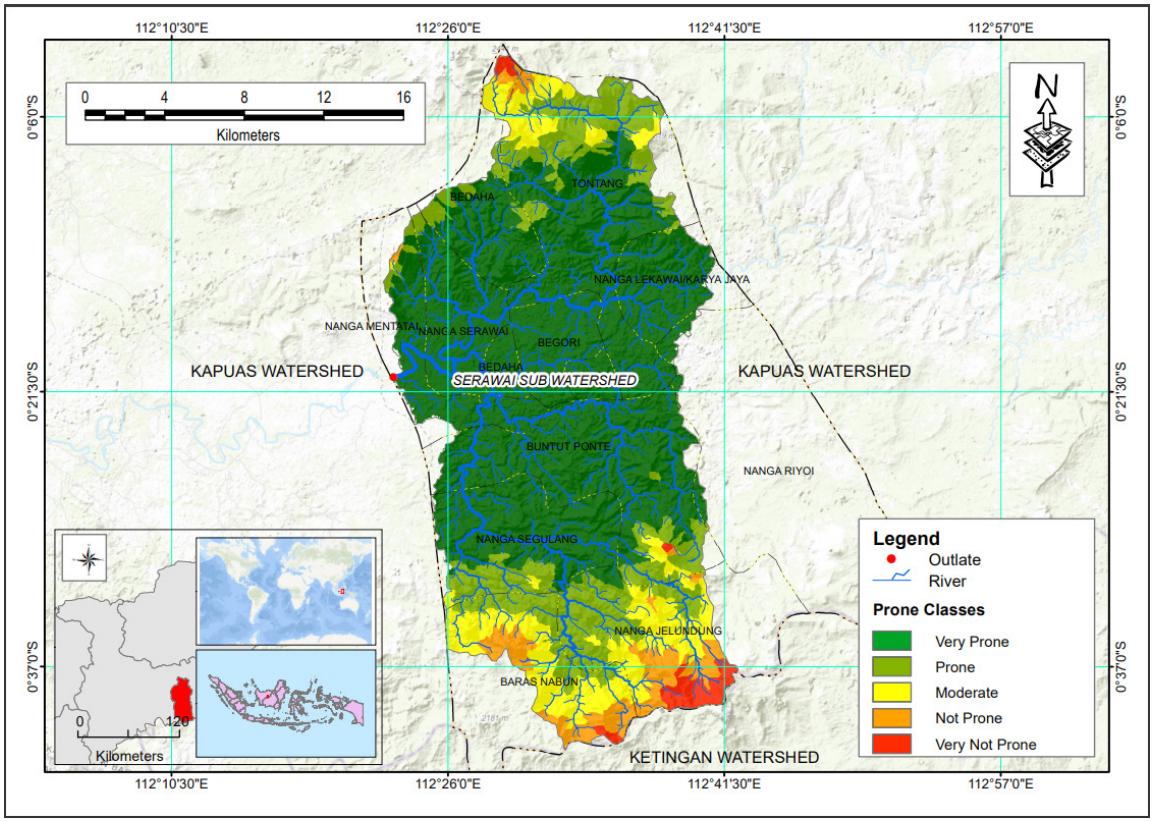

Figure 7. Area and Distribution of Flood Prone

moderate level of prone spread across Tontang village, part of Nanga Jelundung village, and part of Baras Nabun village. The area with a not-prone level, is spread across parts of Baras Nabun and parts of Nanga Jelundung. For areas that are very not prone, spread over parts of the villages of Sedaha, parts of Baras Nabun, and Nanga Jelundung.

HAND is a model and approach for flood-prone mapping developed and validated based on Digital Elevation Model (DEM) data. Without using additional data sources, the current mapping approach may be enhanced by using HAND (Height Above Nearest Drainage) to predict inundation flood areas. The HAND model is a great and straightforward tool for inundation research and inundation area prediction. This model is also advantageous in watersheds without detailed bathymetry or other calibration data.

HAND calculations use the original or modified DEM with a depression removal process. However, this impacts the results related to the flood area, especially for low flood elevations. It is, therefore, advisable to consider DEM without depression. The DEM without depression captures the evenness of the flood profile that runs down the river, accurately depicting the situation on the ground. The estimated area of flood area based on HAND is related to watershed morphology and also the characteristics of the river drainage system.

4. Conclusion

The results showed that the Serawai Sub-watershed has five classes: very prone, prone, moderate, not prone, and very not prone. The very prone class has an area of 112,213.82 ha (65.41%), including Tontang, Sedaha, Nanga Serawai, Begori, Nanga Lekawai, Surga, Buntut Ponte, and Nanga Segulang village. The prone class has an area of 29,356.65 ha (17.14%), spread across the village of part of Beurgea, part of Nanga Segulang, Nanga Jelundung, and part of Tontang village. The moderate level has an area of 18,971.52 ha (11.08%), spread across Tontang, part of Nanga Jelundung, and part of Baras Nabun village. The area with a not-prone is 7,996.20 ha (4.67%), spread across Baras Nabun and parts of Nanga Jelundung village. For areas that are very not prone, they have an area of 3,004.20 (1.75%), spread over parts of the villages of Sedaha, parts of Baras Nabun, and Nanga Jelundung.

Acknowledgment

Thank you to the Directorate General of Higher Education, Research and Technology for funding the research and the Kapuas River Watershed Management Center, West Kalimantan, which has helped a lot in finishing this research.

Reference

Alemayehu, Z. (2007). *Modeling of Flood hazard management for forecasting and emergency response of 'Koka'area within Awash River basin using remote sensing and GIS method*. Addis Ababa University.

Althuwaynee, O. F., Pradhan, B., & Lee, S. (2012). Computers & Geosciences Application of an evidential belief function model in landslide susceptibility mapping. *Computers and Geosciences*, *44*, 120–135. https://doi.org/10.1016/j.cageo.2012.03.003

Barnes, R., Lehman, C., & Mulla, D. (2014). An efficient assignment of drainage direction over flat surfaces in raster digital elevation models. *Computers & Geosciences*, *62*, 128–135.

Basri, H., & Chandra, S. Y. (2021). Assessment of infiltration rate in the Lawe Menggamat Sub-Watershed, Aceh Province, Indonesia. *IOP Conference Series: Earth and Environmental Science*, *667*(1), 12069.

Bui, D. T., Khosravi, K., Shahabi, H., & Daggupati, P. (2019). *Flood Spatial Modeling in Northern Iran Using Remote Sensing and GIS : A Comparison between Evidential Belief Functions and Its Ensemble with a Multivariate Logistic Regression Model*.

Burayu, D. G. (2022). Identification of Groundwater Potential Zones

Using AHP, GIS and RS Integration: A Case Study of Didessa Sub-Basin, Western Ethiopia. *Remote Sensing of Land*, *6 (1)*, 1–15.

Cai, S., Fan, J., & Yang, W. (2021). Flooding Risk Assessment and Analysis Based on GIS and the TFN-AHP Method: A Case Study of Chongqing, China. *Atmosphere*, *12*(5), 623.

Cardoso, C. A., Dias, H. C. T., Soares, C. P. B., & Martins, S. V. (2006). Caracterização morfométrica da bacia hidrográfica do rio Debossan, Nova Friburgo, RJ. *Revista Árvore*, *30*, 241–248.

Cendrero, A., Remondo, J., Beylich, A. A., Cienciala, P., Forte, L. M., Golosov, V. N., Gusarov, A. V, Kijowska-Strugała, M., Laute, K., & Li, D. (2022). Denudation and geomorphic change in the Anthropocene; a global overview. *Earth-Science Reviews*, *233*, 104186.

Choubin, B., Moradi, E., Golshan, M., Adamowski, J., Sajedi-Hosseini, F., & Mosavi, A. (2019). An ensemble prediction of flood susceptibility using multivariate discriminant analysis, classification and regression trees, and support vector machines. *Science of the Total Environment*, *651*, 2087–2096.

Coumou, D., & Rahmstorf, S. (2012). A decade of weather extremes. *Nature Climate Change*, *2*(7), 491–496.

Dantas, A. A. R., & Paz, A. R. (2021). Use of HAND terrain descriptor for estimating flood-prone areas in river basins. *Brazilian Journal of Environmental Sciences (Online)*, *56*(3), 501–516.

Desalegn, H., & Mulu, A. (2021). Flood vulnerability assessment using GIS at Fetam watershed, upper Abbay basin, Ethiopia. *Heliyon*, *7*(1), e05865.

Ekmekcioğlu, Ö., Koc, K., & Özger, M. (2021). Stakeholder perceptions in flood risk assessment: A hybrid fuzzy AHP-TOPSIS approach for Istanbul, Turkey. *International Journal of Disaster Risk Reduction*, *60*, 102327.

Fan, F. M., Collischonn, W., Sorribas, M. V., & Pontes, P. R. M. (2013). Sobre o início da rede de drenagem definida a partir dos modelos digitais de elevação. *Rbrh: Revista Brasileira de Recursos Hídricos. Porto Alegre, RS. Vol. 18, n. 3 (Jul./Set. 2013), p. 241-257*.

Forner, A., Vilana, R., Bianchi, L., Rodríguez-Lope, C., Reig, M., García-Criado, M. Á., Rimola, J., Solé, M., Ayuso, C., & Bru, C. (2015). Lack of arterial hypervascularity at contrast-enhanced ultrasound should not define the priority for diagnostic work-up of nodules< 2 cm. *Journal of Hepatology*, *62*(1), 150–155.

Gentile, N., Lee, E. S., Osterhaus, W., Altomonte, S., Amorim, C. N. D., Ciampi, G., Garcia-Hansen, V., Maskarenj, M., Scorpio, M., & Sibilio, S. (2022). Evaluation of integrated daylighting and electric lighting design projects: Lessons learned from international case studies. *Energy and Buildings*, *268*, 112191.

Geographic, N. (2019). *Floods. Available online:https://www. nationalgeographic.com/environment/ natural-disasters/floods/*.

Gigović, L., Pamučar, D., Bajić, Z., & Drobnjak, S. (2017). Application of GIS-interval rough AHP methodology for flood hazard mapping in urban areas. *Water*, *9*(6), 360.

Goerl, R. F., Michel, G. P., & Kobiyama, M. (2017). Mapeamento de áreas susceptíveis a inundação com o modelo HAND e análise do seu desempenho em diferentes resoluções espaciais. *Revista Brasileira de Cartografia*, *69*(1).

Gorczyca, G., Tylingo, R., Szweda, P., Augustin, E., Sadowska, M., & Milewski, S. (2014). Preparation and characterization of genipin cross-linked porous chitosan–collagen–gelatin scaffolds using chitosan–CO2 solution. *Carbohydrate Polymers*, *102*, 901–911.

Grayson, R. B., & Ladson, A. R. (1991). *DIGITAL TERRAIN MODELLING : A REVIEW OF HYDROLOGICAL , GEOMORPHOLOGICAL , AND BIOLOGICAL APPLICATIONS*. *5*(September 1990), 3–30.

Hagos, Y. G., Andualem, T. G., Yibeltal, M., & Mengie, M. A. (2022). Flood hazard assessment and mapping using GIS integrated with multi-criteria decision analysis in upper Awash River basin, Ethiopia. *Applied Water Science*, *12*(7), 1–18.

Haq, M., Akhtar, M., Muhammad, S., Paras, S., & Rahmatullah, J. (2012). Techniques of remote sensing and GIS for flood monitoring and damage assessment: a case study of Sindh province, Pakistan. *The Egyptian Journal of Remote Sensing and Space Science*, *15*(2), 135–141.

Hu, A., & Demir, I. (2021). Real-time flood mapping on client-side web systems using hand model. *Hydrology*. https://www.mdpi.com/1067816

Huong, H. T. L., & Pathirana, A. (2013). Urbanization and climate change impacts on future urban flooding in Can Tho city, Vietnam. *Hydrology and Earth System Sciences*, *17*(1), 379.

Jenson, S. K., & Domingue, J. O. (1988). Extracting topographic structure from digital elevation data for geographic information system analysis. *Photogrammetric Engineering and Remote Sensing*, *54*(11), 1593–1600.

Jha, A., Lamond, J., Bloch, R., Bhattacharya, N., Lopez, A., Papachristodoulou, N., Bird, A., Proverbs, D., Davies, J., & Barker, R. (2011). Five feet high and rising: cities and flooding in the 21st century. *World Bank Policy Research Working Paper*, *5648*.

Kia, M. B., Pirasteh, S., Pradhan, B., Mahmud, A. R., Nor, W., Sulaiman, A., & Moradi, A. (2012). *An artificial neural network model for flood simulation using GIS : Johor River Basin , Malaysia*. 251–264. https://doi.org/10.1007/s12665-011-1504-z

Komolafe, A. A., Awe, B. S., Olorunfemi, I. E., & Oguntunde, P. G. (2020). Modelling flood-prone area and vulnerability using integration of multi-criteria analysis and HAND model in the Ogun River Basin, Nigeria. *Hydrological Sciences Journal*, *65*(10), 1766–1783.

Kumar, A., Sharma, S., Goyal, N., Singh, A., Cheng, X., & Singh, P. (2021). Secure and energy-efficient smart building architecture with emerging technology IoT. *Computer Communications*, *176*, 207–217.

Lindsay, J. B. (2016). The practice of DEM stream burning revisited. *Earth Surface Processes and Landforms*, *41*(5), 658–668.

Liu, J., Gao, G., Wang, S., Jiao, L., Wu, X., & Fu, B. (2018). The effects of vegetation on runoff and soil loss: Multidimensional structure analysis and scale characteristics. *Journal of Geographical Sciences*, *28*(1), 59–78.

Liu, Y., Cui, Z., Huang, Z., López-Vicente, M., & Wu, G.-L. (2019). Influence of soil moisture and plant roots on the soil infiltration capacity at different stages in arid grasslands of China. *Catena*, *182*, 104147.

Mark, D. M. (1984). Part 4: mathematical, algorithmic and data structure issues: automated detection of drainage networks from digital elevation models. *Cartographica: The International Journal for Geographic Information and Geovisualization*, *21*(2–3), 168–178.

Mehr, A. D., & Akdegirmen, O. (2021). Estimation of urban imperviousness and its impacts on flashfloods in Gazipaşa, Turkey. *Knowledge-Based Engineering and Sciences*, *2*(1), 9–17.

Mojaddadi, H., Pradhan, B., Nampak, H., Ahmad, N., & Halim, A. (2017). *Ensemble machine-learning-based geospatial approach for flood risk assessment using multi-sensor remote-sensing data and GIS*. *5705*(March). https://doi.org/10.1080/19475705.2017.1294113

Momo, M. R., Pinheiro, A., Severo, D. L., Cuartas, L. A., & Nobre, A. D. (2016). Desempenho do modelo HAND no mapeamento de áreas suscetíveis à inundação usando dados de alta resolução espacial. *RBRH*, *21*, 200–208.

Mukherjee, F., & Singh, D. (2020). Detecting flood-prone areas in Harris County: A GIS-based analysis. *GeoJournal*. https://doi.org/10.1007/s10708-019-09984-2

Mumbai, G. (2020). Frequency ratio and fuzzy gamma operator models in GIS : a case study of Urban flood susceptibility zonation mapping using evidential belief function, frequency ratio, and fuzzy gamma operator models in GIS : a case study

of Greater Mumbai, Maharashtra, *Geocarto International*, *0*(0), 1–26. https://doi.org/10.1080/10106049.2020.1730448

Nahib, I., Ambarwulan, W., Rahadiati, A., Munajati, S. L., Prihanto, Y., Suryanta, J., Turmudi, T., & Nuswantoro, A. C. (2021). Assessment of the impacts of climate and LULC changes on the water yield in the Citarum River Basin, West Java Province, Indonesia. *Sustainability*, *13*(7), 3919.

Nobre, A. D., Cuartas, L. A., Hodnett, M., Rennó, C. D., Rodrigues, G., Silveira, A., & Saleska, S. (2011). Height Above the Nearest Drainage–a hydrologically relevant new terrain model. *Journal of Hydrology*, *404*(1–2), 13–29.

Ozkan, S. P., & Tarhan, C. (2016). Detection of flood hazard in urban areas using GIS: Izmir case. *Procedia Technology*, *22*, 373–381.

Prokop, P., Wiejaczka, Ł., Sarkar, S., Bryndal, T., Bucała-Hrabia, A., Kroczak, R., Soja, R., & Płaczkowska, E. (2020). Morphological and sedimentological responses of small stream channels to extreme rainfall and land use in the Darjeeling Himalayas. *Catena*, *188*, 104444.

Purwanto, A., & Andrasmoro, D. (2023). Identification of Groundwater Potential Zones Using Remote Sensing and GIS Technique: A Case Study of the Ketungau Basin in Sintang, West Kalimantan. *The Indonesian Journal of Geography*, *55*(2), 221–234.

Purwanto, A., Rustam, R., Andrasmoro, D., & Eviliyanto, E. (2022). Flood Risk Mapping Using GIS and Multi-Criteria Analysis at Nanga Pinoh West Kalimantan Area. *Indonesian Journal of Geography*, *54*(3).

Rączkowska, Z., Bucała-Hrabia, A., & Kędzia, S. (2024). Triggers of major floods and controls on their geomorphological effects in high-mountain streams (Tatra Mountains, Poland). *CATENA*, *239*, 107933.

Rimba, A. B., Setiawati, M. D., Sambah, A. B., & Miura, F. (2017). Physical flood vulnerability mapping applying geospatial techniques in Okazaki City, Aichi Prefecture, Japan. *Urban Science*, *1*(1), 7.

Rincón, D., Khan, U. T., & Armenakis, C. (2018). Flood risk mapping using GIS and multi-criteria analysis: A greater Toronto area case study. *Geosciences*, *8*(8), 275.

Romanescu, G., Hapciuc, O. E., Minea, I., & Iosub, M. (2018). Flood vulnerability assessment in the mountain–plateau transition zone: a case study of Marginea village (Romania). *Journal of Flood Risk Management*, *11*, S502–S513.

Rozalis, S., Morin, E., Yair, Y., & Price, C. (2010). Flash flood prediction using an uncalibrated hydrological model and radar rainfall data in a Mediterranean watershed under changing hydrological conditions. *Journal of Hydrology*, *394*(1–2), 245–255.

Sahoo, S., Dhar, A., Debsarkar, A., & Kar, A. (2018). Impact of water demand on hydrological regime under climate and LULC change scenarios. *Environmental Earth Sciences*, *77*(9), 341. https://doi.org/10.1007/s12665-018-7531-2

Sajil Kumar, P. J., Elango, L., & Schneider, M. (2022). GIS and AHP Based Groundwater Potential Zones Delineation in Chennai River Basin (CRB), India. *Sustainability*, *14*(3), 1830.

Santos, E. D. S., Pinheiro, H. S. K., & Gallo Junior, H. (2021). Height above the nearest drainage to predict flooding areas in são Luiz do Paraitinga, são Paulo. *Floresta e Ambiente*, *28*, e20200070.

Sarmah, T., Das, S., Narendr, A., & Aithal, B. H. (2020). Assessing human vulnerability to urban flood hazard using the analytic hierarchy process and geographic information system. *International Journal of Disaster Risk Reduction*, *50*, 101659.

Silalahi, F. A., Zainabun, Z., & Basri, H. (2019). Kajian Sifat Fisika Tanah pada Lahan Budidaya Sub DAS Krueng Jreu Kabupaten Aceh Besar. *Jurnal Ilmiah Mahasiswa Pertanian*, *4*(2), 457–463.

Singh, A. P., Arya, A. K., & Singh, D. Sen. (2020). Morphometric analysis of Ghaghara River Basin, India, using SRTM data and GIS. *Journal of the Geological Society of India*, *95*(2), 169–178.

Skilodimou, H. D., Bathrellos, G. D., Chousianitis, K., Youssef, A. M., & Pradhan, B. (2019). Multi-hazard assessment modeling via multi-criteria analysis and GIS: a case study. *Environmental Earth Sciences*, *78*(2), 47.

Speckhann, G. A., Chaffe, P. L. B., & ... (2018). Flood hazard mapping in Southern Brazil: a combination of flow frequency analysis and the HAND model. *Hydrological …*. https://doi.org/10.1080/02626667.2017.1409896

Sugianto, S., Deli, A., Miswar, E., Rusdi, M., & Irham, M. (2022). The effect of land use and land cover changes on flood occurrence in Teunom Watershed, Aceh Jaya. *Land*, *11*(8), 1271.

Suryadi, U. E., & Riduansyah, B. (2021). LAJU INFILTRASI PADA BEBERAPA PENGGUNAAN LAHAN DI DESA PAK MAYAM KECAMATAN NGABANG KABUPATEN LANDAK. *Jurnal Sains Mahasiswa Pertanian*, *10*(1).

Ullah, K., & Zhang, J. (2020). GIS-based flood hazard mapping using relative frequency ratio method: A case study of Panjkora River Basin, eastern Hindu Kush, Pakistan. *Plos One*, *15*(3), e0229153.

Wondim, Y. K. (2016). Flood hazard and risk assessment using GIS and remote sensing in lower Awash sub-basin, Ethiopia. *Journal of Environment and Earth Science*, *6*(9), 69–86.

Wu, T., Li, J., Li, T., Sivakumar, B., Zhang, G., & Wang, G. (2019). High-efficient extraction of drainage networks from digital elevation models constrained by enhanced flow enforcement from known river maps. *Geomorphology*, *340*, 184–201.

Zhang, N., Luo, Y.-J., Chen, X.-Y., Li, Q., Jing, Y.-C., Wang, X., & Feng, C.-H. (2018). Understanding the effects of composition and configuration of land covers on surface runoff in a highly urbanized area. *Ecological Engineering*, *125*, 11–25.

Zhou, Q., Su, J., Arnbjerg-Nielsen, K., Ren, Y., Luo, J., Ye, Z., & Feng, J. (2021). A GIS-Based Hydrological Modeling Approach for Rapid Urban Flood Hazard Assessment. *Water*, *13*(11), 1483.

Zwenzner, H., & Voigt, S. (2009). Improved estimation of flood parameters by combining space-based SAR data with very high-resolution digital elevation data. *Hydrology and Earth System Sciences*, *13*(5), 567–576.